# Ultraviolet and visible resonance-enhanced Raman scattering in epitaxial Al$_{1-x}$In$_x$N thin films

V. M. Naik[a)]
*Department of Natural Sciences, University of Michigan-Dearborn, Dearborn, Michigan 48128*

W. H. Weber and D. Uy
*Scientific Research Laboratory, Ford Motor Company, Dearborn, Michigan 48121*

D. Haddad and R. Naik
*Department of Physics and Astronomy, Wayne State University, Detroit, Michigan 48202*

Y. V. Danylyuk, M. J. Lukitsch, G. W. Auner, and L. Rimai
*Department of Electrical and Computer Engineering, Wayne State University, Detroit, Michigan 48202*

We report the observation of ultraviolet and visible near-resonance enhanced Raman scattering in epitaxial wurtzite Al$_{1-x}$In$_x$N (0001) ($0 \leq x < 0.7$) thin films. The films (thickness~150 nm) were grown by plasma source molecular beam epitaxy on sapphire (0001) substrates. A substantial spectral enhancement is seen for Al-rich samples using 244 nm (5.01 eV) radiation due to the closeness of their band gap energy to the excitation energy. On the other hand, samples with $x \sim 0.6$ (energy band gap $\sim 2.5$ eV) show significant enhancement with 514.5 nm (2.41 eV) excitation. The $A_1$(LO) and $E_2$ zone center phonons have been observed for all the samples. The $A_1$(LO) phonon frequency shows the expected decrease with increasing $x$. The $E_2$ mode shows a two-mode behavior supporting the recent theoretical predictions. Due to increased resonance enhancement, strong second- and third-order spectra are seen in some films. © *2001 American Institute of Physics.* [DOI: 10.1063/1.1404402]

Growing interest in developing optoelectronic devices operating in blue, green, and ultraviolet regions has stimulated the study of nitride ternary alloys: InGaN, AlGaN, and AlInN.[1,2] Alloying among the group III nitrides allows band gap tuning from 1.9 eV in InN to 6.2 eV in AlN with an intermediate value of 3.5 eV for GaN. However, there have been few studies on Al$_{1-x}$In$_x$N films due to the difficulty associated with their growth.[3–8]

The hexagonal wurtzite Al$_{1-x}$In$_x$N system belongs to the space group $C_{6v}^4$ with four atoms in the primitive unit cell. The representation at the $\Gamma$ point is reducible to

$$\Gamma = 1A_1 + 1E_1 + 2E_2 + 2B_1.$$

The $A_1$ and $E_1$ phonon modes are both Raman and infrared active; the $E_2$ modes are Raman active, while $B_1$ modes are silent. The lattice dynamic calculations on Al$_{1-x}$In$_x$N crystals based on the modified random element isodisplacement have been reported by Grille, Schnittler, and Bechstedt[9] Their calculations predict a two-mode behavior for $E_2$ and $E_1$(TO) modes, whereas almost a linear increase with Al concentration for the $A_1$(LO) mode. However, there are no reported experimental Raman scattering data on these alloy films. Here, we report the observation of near-resonance-enhanced Raman scattering in Al$_{1-x}$In$_x$N thin films, using ultraviolet (UV) and visible light excitation (244 and 514.5 nm).

The epitaxial Al$_{1-x}$In$_x$N alloy thin films ($0 \leq x < 0.7$) have been grown on sapphire (0001) substrates using plasma source molecular beam epitaxy.[10] X-ray diffraction (XRD)

$\theta$–$2\theta$ scans of these films confirm wurtzite $c$-plane growth without any alloy segregation. The films are typically 150 nm thick. The energy band gaps of these alloys have been determined using optical transmission and reflection measurements in the UV and near-IR region.[11] These values decrease with increasing $x$, as expected from the band gaps for the end point compounds. The band gap energies for the samples studied in this letter are shown in Table I. The alloy compositions were estimated by (0002) XRD peak positions using Vegard's rule.

The Raman spectra were recorded using two different spectrometers. Micro-Raman measurements were made in backscattering geometry with a Renishaw 1000 system using 244 nm excitation. A single monochromator (Instruments SA-Triax 550), equipped with conventional optics, holographic supernotch filters, and a charge coupled device detector, was used to record spectra using 514.5 nm excitation line. The experimental scattering configuration used in this work allows the detection of $A_1$(LO) and $E_2$ phonons.

Figure 1 shows the Raman spectra of an AlN film, i.e.,

TABLE I. Energy band gaps of Al$_{1-x}$In$_x$N thin films.[a]

| Sample | $x$ | $E_g$ (eV) |
|---|---|---|
| i | 0.00 | $6.00 \pm 0.10$ |
| ii | 0.12 | $4.20 \pm 0.25$ |
| iii | 0.28 | $3.30 \pm 0.10$ |
| iv | 0.34 | $3.20 \pm 0.10$ |
| v | 0.55 | $2.60 \pm 0.15$ |
| vii | 0.67 | $2.50 \pm 0.15$ |

[a]Reference 11.

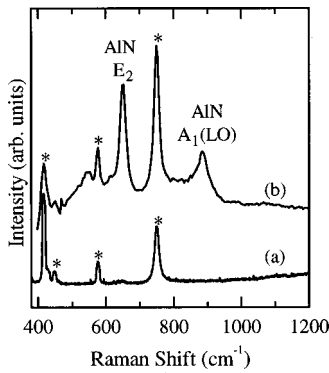[a)]Electronic mail: vmnaik@umich.edu

FIG. 1. Raman spectra of AlN film obtained with (a) 514.5 nm and (b) 244 nm excitation. Trace (a) shows Raman peaks of only sapphire (*), whereas trace (b) shows both AlN and sapphire peaks.



FIG. 3. Raman spectra of sample ($v$) [$x=0.55$] obtained using (a) 514.5 nm excitation and (b) 244 nm excitation. Note the strong enhancement in (a) compared to (b). The alloy peaks are marked with vertical arrows.

sample (i) in Table I, obtained using both visible and UV laser excitations. The lower trace (a) obtained with visible laser excitation (514.5 nm) shows only the phonon modes of the sapphire substrate without any Raman signal from AlN. On the other hand, trace (b) obtained using UV laser excitation (244 nm) shows strong enhancement of the Raman modes from AlN. The $A_1$(LO) and $E_2$ phonons of AlN are clearly identified and their energies are 884 and 653 cm$^{-1}$. However, these observed frequencies are 6 and 4 cm$^{-1}$ lower than those for bulk (strain free) AlN,[12,13] perhaps indicating a small tensile strain in the film.

Figure 2 shows the Raman spectra of samples (ii)–(v) obtained with 244 nm excitation. Sample (ii) [Fig. 2(a)] shows strongly enhanced $A_1$(LO) at 859 cm$^{-1}$ and two $E_2$ modes at 677 and 627 cm$^{-1}$. Samples (iii) and (iv) show $A_1$(LO) and $E_2$ modes that shift downward in frequency with increasing $x$. However, the intensity enhancement in these samples is considerably reduced. Further, no discernible peaks are observed in samples (v) and (vi) due to the much lower band gap energy ($\sim 2.5$ eV) of these samples compared to the excitation line. Samples (ii), (iii), and (iv)
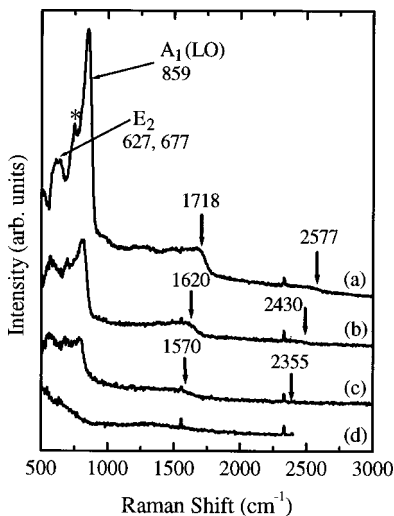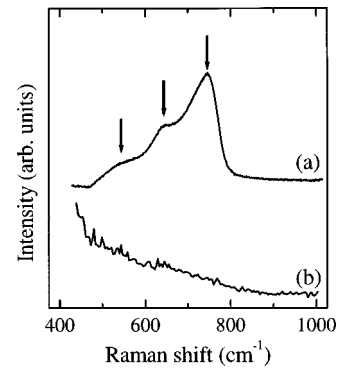
also show distinct steps at frequencies corresponding to twice and three times their $A_1$(LO) frequencies, which are indicated by the vertical arrows in Fig. 2. These steps arise from the cutoffs in the second- and third-order Raman scattering, and they appear at multiples of the $A_1$(LO) mode, since that mode is near the top of the phonon bands. The strength of these cutoff features is another indication of the strong resonance enhancement that occurs with near-band gap excitation.

Raman spectra of all samples were also recorded with 514.5 nm excitation. While Al-rich samples ($x \leq 0.34$) showed only sapphire peaks, samples (v) and (vi) showed strong Raman signals due to the closeness of their energy band gap ($\sim 2.5$ eV) to the excitation energy (2.41 eV). For example, Fig. 3 shows the Raman spectra of sample (v) obtained using both visible [trace (a)] and UV excitation [trace (b)]. Strongly enhanced $A_1$(LO) at 743 cm$^{-1}$ and two $E_2$ modes at 648 and 560 cm$^{-1}$ are seen. The Raman data from the samples listed in Table I are plotted in Fig. 4.

Figure 4 shows the comparison of Raman frequencies of $Al_{1-x}In_xN$ samples studied in this work with the theoretical predictions of the zone-center phonons versus composition ($x$) in $2H$-$Al_{1-x}In_xN$ alloys.[9] The $A_1$(LO) phonon clearly follows the predicted behavior. An important phenomenon in alloyed semiconductor systems of the form $A_{1-y}B_yC$ relates to the behavior of the frequencies of the long wavelength optical phonons with changing concentration $y$. In these mixed crystals, there are two types of observed behavior
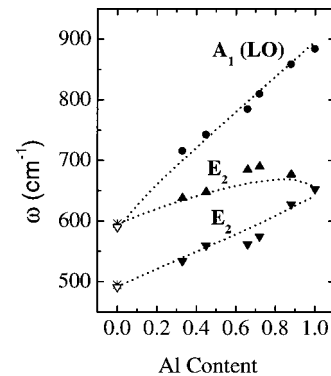


FIG. 2. Raman spectra of 150-nm-thick $Al_{1-x}In_xN$ samples obtained using 244 nm excitation: (a) $x=0.12$, (b) $x=0.28$, (c) $x=0.34$, (d) $x=0.55$. Note the strong enhancement in (a) and (b). The second- and third-order features are seen in (a), (b), and (c). The vertical lines are drawn at two and three times the measured $A_1$(LO) frequency. Raman peak of sapphire is indicated by *.



FIG. 4. Zone-center phonon frequencies vs Al content of $Al_{1-x}In_xN$. The symbols represent the data obtained in the present work. The dotted lines represent theory (Ref. 9). For InN the data are from Refs. 15 and 16.

upon alloying. In the one-mode class the frequencies vary continuously and approximately linearly with $y$, whereas in the two-mode behavior, two sets of frequencies corresponding approximately to those in pure AC and BC are observed throughout the alloying range. Grille and co-workers have performed the lattice dynamical calculations on the $Al_{1-x}In_xN$ alloy system and the results indicate that $E_2$ and $E_1(TO)$ modes show a two-mode behavior. We clearly observe two-mode behavior for $E_2$ phonons. We cannot detect the $E_1(TO)$ in the scattering geometry used here. Figure 4 shows the experimentally observed $E_2$ modes are in good agreement with the theoretical predictions. The splitting of two $E_2$ modes in Al-rich samples (iii) and (iv) is somewhat larger than predicted by theory. Perhaps, this may be due to the strain in these films. It is possible that the phase separation is suppressed, particularly in the Al-rich alloy films, due to strain. Indeed, theoretically it has been shown that the phase separation is suppressed due to strain in the case of cubic $In_xGa_{1-x}N$ alloys.[14]

To summarize, we present the observation of first- and higher-order Raman scattering in epitaxial wurtzite $Al_{1-x}In_xN$ (0001) ($0 \leq x < 0.7$) thin films using UV and visible excitations. $A_1(LO)$ and $E_2$ zone center phonons have been observed as a function of Al composition. The $A_1(LO)$ phonon frequency shows the expected increase with increasing Al concentration. The $E_2$ mode shows a two-mode behavior supporting the recent theoretical predictions. Due to increased resonance enhancement, strong second- and third-order spectra have been observed in some films.

[1] S. C. Jain, M. Willander, J. Narayan, and R. Van Overstraeten, J. Appl. Phys. **87**, 965 (2000).

[2] S. Nakamura, *The Blue Laser Diode-GAN Based Light Emitters and Lasers* (Springer, Berlin, 1997).

[3] S. Yamaguchi, M. Kariya, S. Nitta, T. Takeuchi, C. Wetzel, H. Amano, and I. Akasaki, Appl. Phys. Lett. **76**, 876 (2000), and references therein.

[4] T. Peng, J. Piprek, G. Qiu, J. O. Olowoiafe, K. M. Unruh, C. P. Swann, and E. F. Shubert, Appl. Phys. Lett. **71**, 2439 (1997).

[5] K. S. Kim, A. Saxler, P. Kung, M. Razaghi, and K. Y. Lim, Appl. Phys. Lett. **71**, 800 (1997).

[6] O. Guo, H. Ogawa, and A. Yoshida, J. Cryst. Growth **146**, 462 (1995).

[7] K. Kubota, Y. Kobayashi, and K. Fujimoto, J. Appl. Phys. **66**, 2984 (1989).

[8] T. Matsuoka, Appl. Phys. Lett. **71**, 105 (1997).

[9] H. Grille, Ch. Schnittler, and F. Bechstedt, Phys. Rev. B **61**, 6091 (2000).

[10] M. J. Lukitsch, G. W. Auner, R. Naik, and V. M. Naik, Mater. Res. Soc. Symp. Proc. **639**, G6.29.1 (2001).

[11] Y. V. Danylyuk, M. J. Lukitsch, C. Huang, G. W. Auner, R. Naik, and V. M. Naik, Mater. Res. Soc. Symp. Proc. **639**, G6.54.1 (2001).

[12] J. M. Hays, M. Kuball, Y. Shi, and J. H. Edgar, Jpn. J. Appl. Phys., Part 2 **39**, L710 (2000).

[13] L. Bergman, M. Dutta, and R. J. Nemanich, in *Raman Scattering in Materials Science*, edited by W. H. Weber and R. Merlin (Springer, Berlin, 2000).

[14] I. K. Teles, J. Furthüller, L. M. Scolfaro, J. R. Leite, and F. Bechstedt, Phys. Rev. B **62**, 2475 (2000).

[15] M. C. Lee, H. C. Lin, Y. C. Pan, C. K. Shu, J. Ou, W. H. Chen, and W. K. Chen, Appl. Phys. Lett. **73**, 2606 (1998).

[16] G. Kaczmarczyk A. Kaschner, S. Reich, A. Hoffman, C. Thomsen, D. J. As, A. P. Lima, D. Schikora, K. Lischka, R. Averbeck, and H. Riechert, Appl. Phys. Lett. **76**, 2122 (2000).